NIPPON STEEL TECHNICAL REPORT No. 124 SEPTEMBER 2020

Technical Report

UDC 669 . 184 . 244 . 66 : 620 . 192 . 45

Effect of Particle Velocity on Penetration and Flotation Behavior

Akihiro MATSUZAWA* Katsuhiro SASAI
Hiroshi HARADA Mitsuhiro NUMATA

Abstract

As a fundamental investigation to improve reaction efficiency in the powder blasting process, the effects of particle velocity on penetration and flotation behavior were examined by the water model experiment. A single particle was blasted onto the water surface with Ar gas, and the behavior of the particle was recorded by a high-speed camera. Due to penetration of the particle, an air column was generated and a residual bubble remained on the particle after rupture of the air column. In the case that particle velocity before penetration was low, the detention time of the particle increases with the increase in the maximum penetration depth. In the case that particle velocity before penetration was high, detention time did not increase as much with the increase in the maximum penetration depth because the diameter of the residual bubble and buoyancy became large. To prevent the generation of a residual bubble, the particle should be penetrated with a velocity that does not generate an air column.

1. Introduction

A lower sulfur concentration of steel is required because demand for improvement of steel properties is increasing. Therefore, improving the efficiency of dephosphorization and desulfurization treatment is one of the most important tasks in the refining process. Desulfurization treatment for low sulfur steel is often operated in secondary refining processes, such as vacuum degassing (RH) and ladle furnace (LF), and powder blasting is often carried out in the RH process. In this process, refining reagent particles are blasted onto the surface of molten steel in a vacuum vessel. These particles penetrate and disperse into the molten steel. Then, these particles transfer from the down-leg to the ladle due to circulation of the molten steel and float in the ladle. After that, most of the particles are absorbed by the ladle slag. It is considered that effective penetration of refining reagent particles into molten steel and their dispersion are important to improve the reaction efficiency because the surface tension of molten steel is large and the difference in density between the molten steel and refining reagent particles is also large.

Many researches on the penetration behavior of particles can be classified into two broad groups. One includes experiments using fine powder, while the other involves experiments using a single particle with a relatively large diameter.

The main purpose of the former group is to clarify the penetration behavior from a macroscopic perspective. For example, Engh et al.[1] suggested an empirical formula of penetration depth by a water model experiment, and Kimura[2] reported that the penetration mode differed according to the powder blasting condition. Also, the estimation of mass transfer velocity in powder blasting has been reported recently.[3] Furthermore, for powder injection processes into liquid, Narita et al.[4] reported the penetration and dispersion behavior of powder, and Oda et al.[5] evaluated the effect of wettability (contact angle) and the diameter of a particle on the penetration ratio.

On the other hand, the main purpose of the latter group is to clarify the penetration behavior in detail. For example, Ozawa et al.[6] carried out experiments where a particle, such as glass, was dropped onto a mercury surface and suggested the critical condition of particle penetration into liquid as a critical Weber number. Also, Lee et al.[7] carried out a water model experiment by blasting a polystyrene particle onto the water surface, analyzed the relation between the particle penetration velocity and penetration depth, and concluded that most of the kinetic energy of the particle was lost by air column generation. Furthermore, Shimamoto et al.[8] and Tanaka et al.[9] carried out water model experiments where a single particle was dropped onto the water surface, and the phenomenon of particle penetration into the liquid was observed and analyzed. According to Shimamoto et al., an air column is generated by the particle penetra-

* Senior Researcher, Muroran R & D Lab.
12 Nakamachi, Muroran City, Hokkaido 050-8550

tion and deformation of the water surface. Then, a part of the ruptured air column remains on the particle surface and becomes a residual bubble.

Thus many experimental results on the critical penetration condition and maximum penetration depth of a particle have been reported. However, there are no reports on to what extent the time during which a particle remains in liquid (detention time) changes as the maximum penetration depth increases. Therefore, in this study, a water model experiment to blast a single particle onto the water surface was carried out. Then, the relation between the maximum penetration depth and detention time of the particle was analyzed.

2. Experimental Procedures

A schematic view of the experimental apparatus is shown in **Fig. 1**. It is made of transparent acrylic resin and the vacuum vessel (inner size is 280 mm in height, 180 mm in width, and 90 mm in depth) is rectangular to avoid distortion caused by refraction. This apparatus has a close-packed structure including a water bath to reduce the pressure in the vessel. Valves installed on the upper plate of the vacuum vessel were used to discharge air and blow gas in.

The experimental procedures are as follows. A predetermined amount of Ar gas was inserted into the vessel through a single-hole straight nozzle (5 mm in inner diameter) which was set at the center of the upper plate of the vessel. The length of the nozzle was 70 mm or 140 mm and the water depth in the vessel before reducing the pressure was 80 mm. The pressure in the vessel was reduced by a vacuum pump and maintained at 52 kPa by a vacuum regulator. The water depth in the vessel increased to 84 mm as a result of the pressure reduction. Then, valve-B was closed and a single particle (polypropylene, 910 kg/m^3 in density, 3.2 mm in diameter) was kept between valve-A and valve-B. Next, valve-B was opened with valve-A closed. The particle was dropped through the nozzle and blasted onto the water surface of the vessel with Ar gas. The behavior of the particle was recorded by a high-speed camera (250 frames/s) and changes in the penetration depth of the particle over time were analyzed by the equation which converts the length on the monitor of the camera to the actual length. The converting equation was obtained by preliminary experiments.

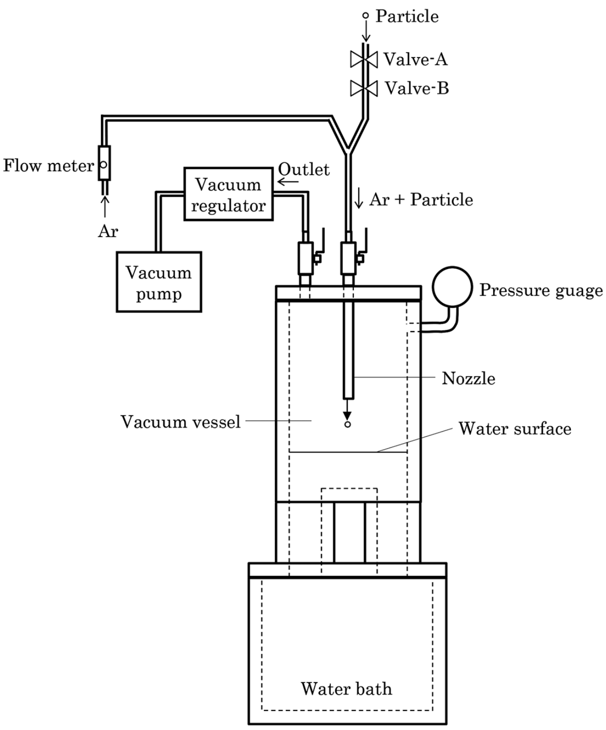

Fig. 1 Experimental apparatus

The experimental conditions are shown in **Table 1**. The Ar flow rate, Q_{Ar}, and nozzle gap, h (distance from the static water surface to the tip of the nozzle) were varied to provide ten different conditions. Experiments were carried out three times in each condition.

The particle velocity before penetration to the water surface was measured in another experiment. A particle discharged from the nozzle was recorded by a high-speed camera (1 000 frames/s), and the particle velocity was calculated from the transport distance between two frames (0.001 s) just before the penetration to the water surface. The particle velocities before the penetration are listed in Table 1.

3. Experimental Results and Discussion

3.1 Change of penetration depth of a particle over time

Recorded pictures in the case of D2 (particle velocity before the penetration: 6.7 m/s) are shown in **Fig. 2** as an example of the penetration and flotation behavior of a particle. The water surface was deformed by the particle penetration and an air column was generated. When the air column was ruptured, a part of the air column remained on the particle and became a residual bubble. After the rupture of the air column, the particle penetrated to the maximum depth and then floated to the water surface.

However, in some conditions where the particle velocity before the penetration is low, such as the case of A2 (particle velocity before the penetration: 1.1 m/s), the particle penetrated without generating either an air column or a residual bubble as shown in **Fig. 3**.

Changes in the penetration depth over time are shown in **Fig. 4**. Although the penetration was the deepest in the case of E2, the time from the penetration to the flotation to the water surface was the longest in the case of B1.

The values measured from the pictures taken by the high-speed camera are shown in **Fig. 5**. (a) The particle velocity after the penetration was calculated by the transfer distance between two frames (0.004 s) just after the penetration to the water surface. (b) The maximum air column length, H_{max}, was defined as the distance from the base point to the upper side of the particle just before the air column

Table 1 Experimental conditions

No.	Ar gas flow rate Q_{Ar} (NL/min)	Nozzle length (mm)	Nozzle gap h (mm)	Particle velocity before penetration (m/s)
A1	0	70	126	1.7
A2	0	140	56	1.1
B1	5	70	126	2.5
B2	5	140	56	3.4
C1	10	70	126	3.4
C2	10	140	56	5.0
D1	15	70	126	5.9
D2	15	140	56	6.7
E1	25	70	126	7.2
E2	25	140	56	10.9

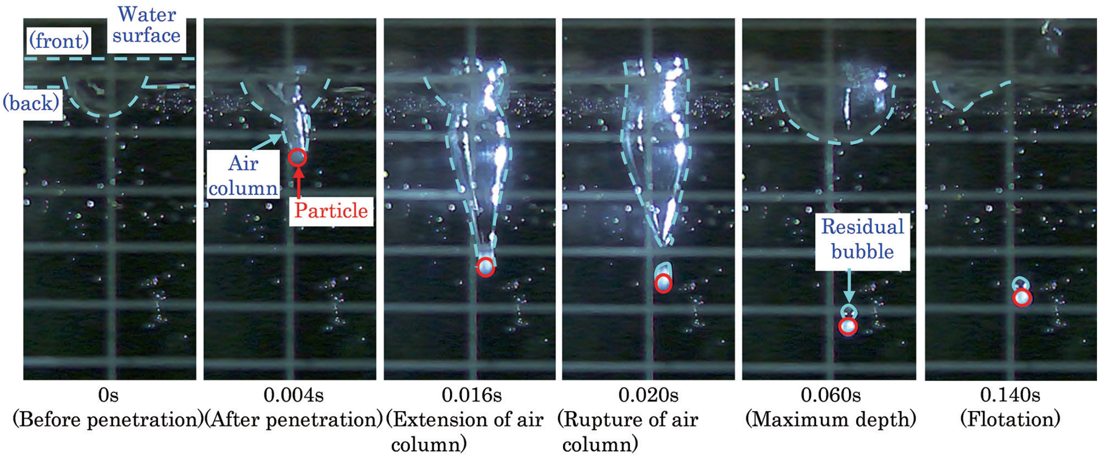

Fig. 2 Penetration and flotation behavior of a particle (D2)

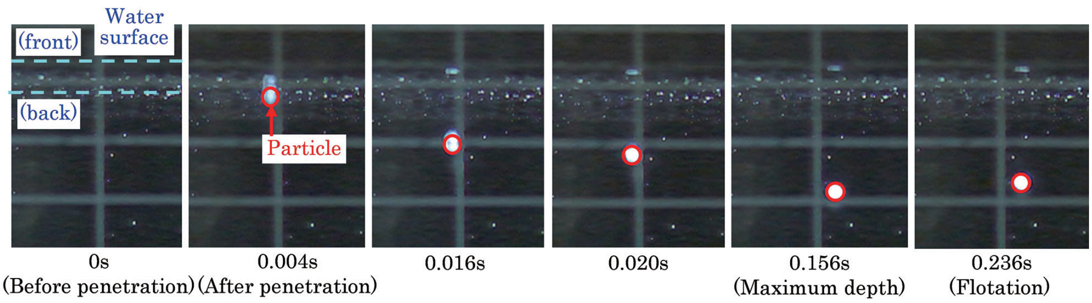

Fig. 3 Penetration and flotation behavior of a particle (A2)

rupture, and (c) the maximum penetration depth, L_{max}, was defined as the distance from the base point to the center of the particle at the maximum depth. The base point means the depth of a cavity on the water surface before the penetration. (d) The diameter of the residual bubble, d_B, was measured at the moment when the shape of the bubble remaining on the water surface became almost spherical. (e) The average flotation velocity was obtained by linear regression calculation of the particle depth over time during the period that the particle flotation velocity became almost constant. (f) The detention time of the particle was defined as the period from the air column rupture to the flotation to the water surface. In some conditions, the particles were hidden behind the cavities before reaching the water surface. Therefore, the detention time was calculated by extrapolating the particle depth to the water surface during the flotation.

In this experiment, there were some cases where the particle did not penetrate in the vertical direction and its orbit bent widely to the horizontal direction after the penetration. In these cases, the maximum penetration depth became smaller than the case where the particle penetrated in the vertical direction. These cases were excluded from the analysis because the maximum depth position deviated by 20° or more in the horizontal direction from the penetration position on the water surface.

3.2 Particle velocity after penetration

A comparison of particle velocity after penetration with that before penetration is shown in **Fig. 6**. The particle velocity after penetration was 0.7 to 3.4 m/s while the particle velocity before penetration was 1.1 to 10.9 m/s, and it did not increase as much as the particle velocity before penetration increased. This indicates that the kinetic energy of the particle is largely lost by penetration of the water surface.

3.3 Maximum air column length and maximum penetration depth

The effect of the particle velocity before penetration on the maximum air column length, H_{max}, is shown in **Fig. 7**. $H_{max} = 0$ mm means that no air column was generated, and it was caused by lower particle velocity than 3.4 m/s before penetration under our study conditions. Also, H_{max} increased with the increase in particle velocity before penetration in the case that the particle velocity before penetration was higher than 3.4 m/s.

With regards to the collision of a particle with a liquid surface, it is hypoethisized[10, 11] that a liquid film spreads along the particle surface (progress of wetting) and an air column is generated in the case that the particle velocity is higher than the moving velocity of the liquid film. In this experiment, the moving velocity of the liquid film does not differ among all conditions because the wettability between the particle and liquid is the same. Therefore, an air column is generated in the conditions where the particle velocity before penetration is higher than the criterion velocity.

The effect of the particle velocity before the penetration on the maximum penetration depth, L_{max}, is shown in **Fig. 8**. L_{max} increased as the particle velocity before penetration increased as is the case with H_{max}. The maximum penetration depth varies even when the blasting condition is the same. Possible reasons are the friction between the particle and the inner wall of the nozzle when the particle passes through the nozzle, penetration angle of the particle to the water surface, consumption of a part of the kinetic energy of the particle by its rotation, and so forth.

According to Ozawa et al.,[6] the kinetic equation of a particle passing through the gas-liquid interface vertically is given by Equation (1). The first term on the right side is the liquid drag force, the

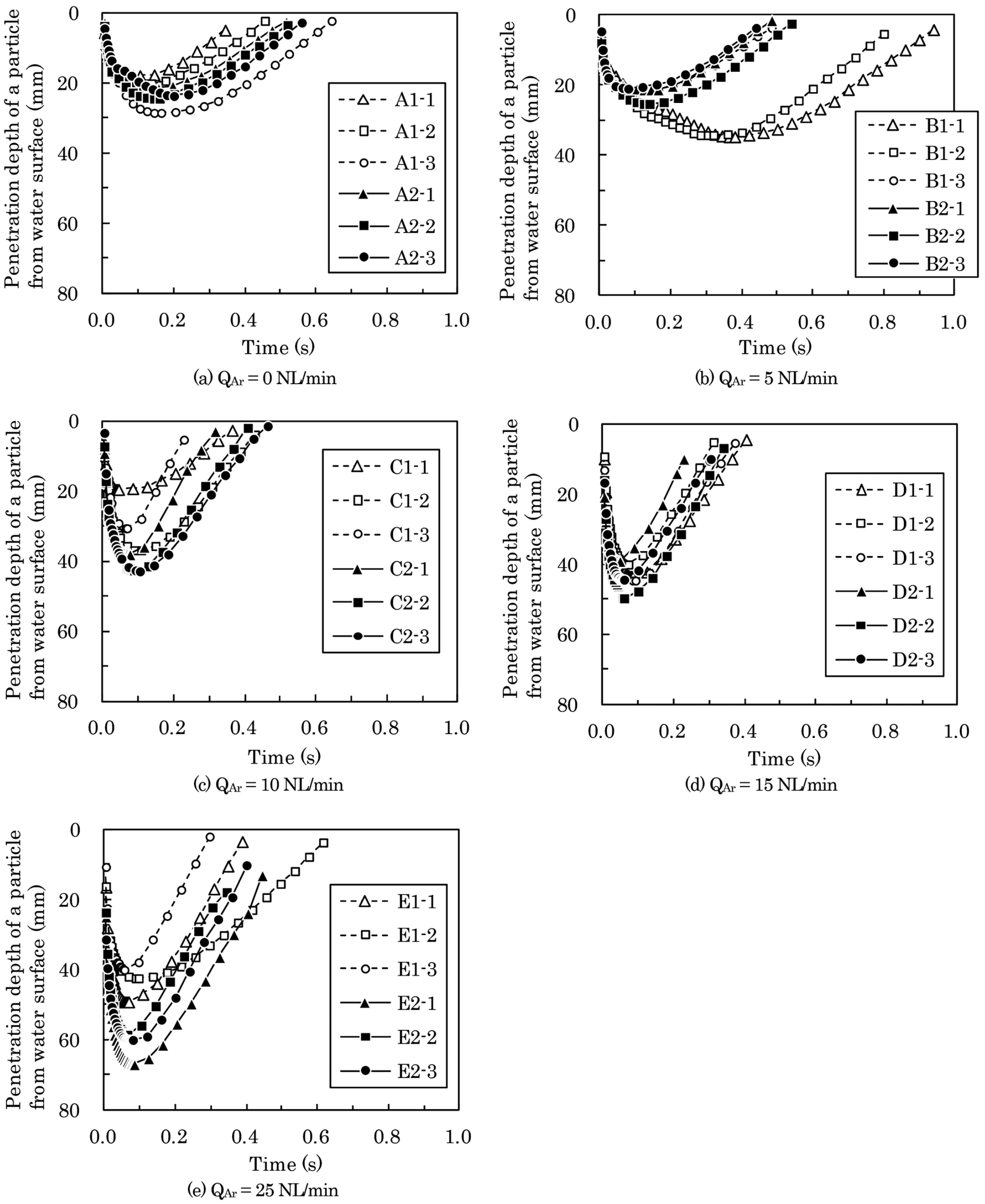

Fig. 4 Change of penetration depth of a particle from water surface with time

second term is the gravity force, the third term is the buoyancy force, and the fourth term is the force caused by the interfacial tension.

$$-\frac{dv_P}{dt}\left(\frac{4}{3}\pi r_P^3\rho_P+\alpha\cdot\frac{4}{3}\pi r_P^3\rho_L\right)=\pi r_P^2\cdot\frac{1}{2}\rho_L v_P^2 C_D\cdot\phi_1\left(\frac{x}{r_P}\right)-\frac{4}{3}\pi r_P^3\rho_P g+\frac{4}{3}\pi r_P^3\rho_L g\cdot\phi_2\left(\frac{x}{r_P}\right)+2\pi r_P\sigma_{GL}\cdot\phi_3\left(\frac{x}{r_P}\right) \qquad (1)$$

Where, v_P is the particle velocity (m/s), t is the time (s), r_P is the radius of the particle (m), ρ_P is the density of the particle (kg/m^3), ρ_L is the density of the liquid (kg/m^3), C_D is the drag coefficient (-), x is the penetration depth of the particle into the liquid (m), g is the gravitational acceleration (m/s^2), and σ_{GL} is the surface tension of the liquid (N/m). Also, α is a coefficient related to the imaginary mass (-), and $\phi_1(x/r_P)$, $\phi_2(x/r_P)$, and $\phi_3(x/r_P)$ are correction coefficients related to the drag coefficient C_D, buoyancy force, and surface tension, respectively.

Equation (2) is obtained by transformation of Equation (1), replacing x/r_P with x^*, ρ_P/ρ_L with ρ^*, $\phi_1(x^*)$ with constant ϕ_1, $\phi_2(x^*)$ with constant ϕ_2, $\phi_3(x^*)$ with $A(x^*-1-\cos\theta)$, ρ_a^* with $\rho^*+\alpha$, and ρ_b^* with $\rho^*-\phi_2$, where θ is the contact angle (°), and A is a proportional coefficient of the interfacial tension by generating a cavity on the liquid surface.

$$\frac{dv_P^2}{dx^*}+\frac{3C_D\phi_1}{4\rho_a^*}v_P^2=-\frac{3A\sigma_{GL}}{r_P\rho_L\rho_a^*}x^*+\frac{2r_P g\rho_b^*}{\rho_a^*}+\frac{3A\sigma_{GL}}{r_P\rho_L\rho_a^*}(1+\cos\theta) \qquad (2)$$

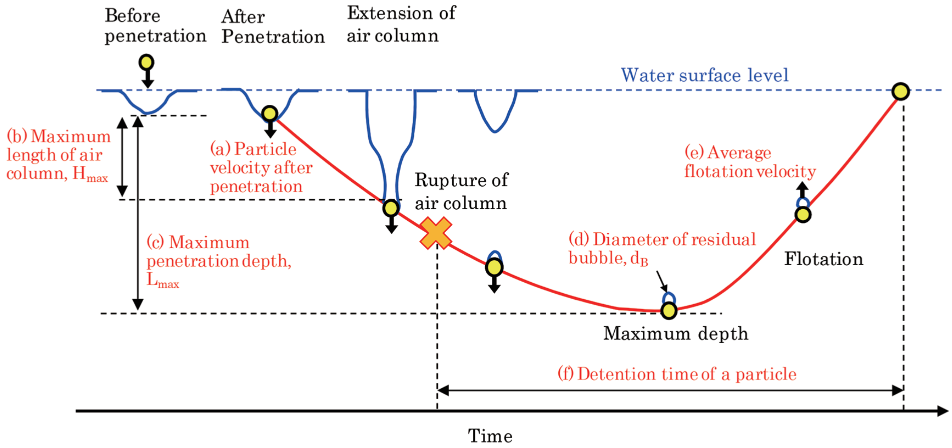

Fig. 5 Schematic diagram of a particle behavior and analyzed factors in present work

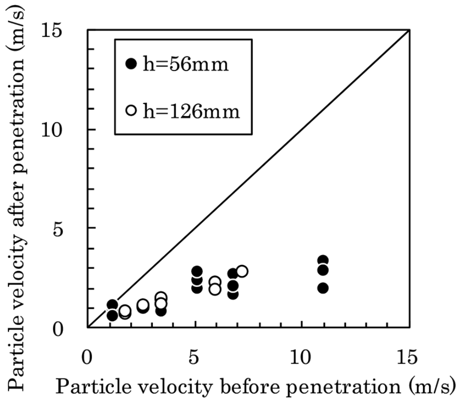

Fig. 6 Comparison of particle velocity after penetration with that of before penetration

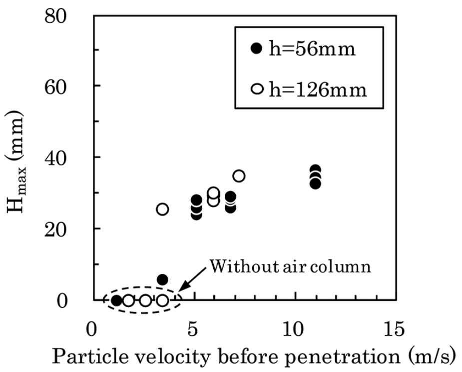

Fig. 7 Effect of particle velocity before penetration on maximum length of air column

Thus, more than half of the maximum penetration depth consisted of an air column. Therefore, similarly to the approach by Ozawa et al., α was defined as 0.25, ϕ_1 as 1, ϕ_2 as 0.5, and A as 2.5, based on the assumption that a half part of the particle was dipped into the liquid. Also, the drag coefficient C_D was defined as 0.44, gravitational acceleration g as 9.8 m/s^2, density of water ρ_L as 1 000 kg/m^3, surface tension of water σ_{GL} as 0.073 N/m,[12] and the contact angle between the polypropylene and water θ as 95°.[13]

When the particle velocity before penetration is v_{P0} (m/s), v_P is v_{P0} when x^* is 0. When this critical condition is used to solve Equation (2) in terms of v_P^2 and when v_P is 0 in the case that the maximum penetration depth x^* is L_{max}^* $(=L_{max}/r_P)$, Equation (3) is obtained.

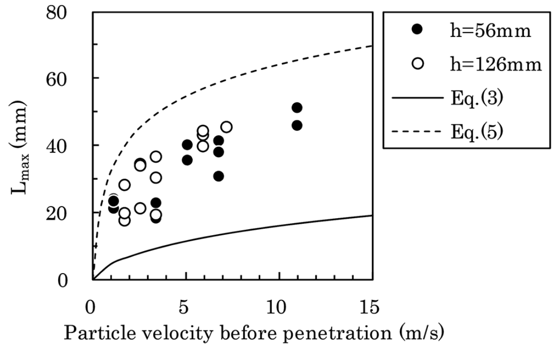

Fig. 8 Effect of particle velocity before penetration on maximum penetration depth

$$v_{P0}^2 \cdot \exp\left(-\frac{3C_D\phi_1}{4\rho_a^*}L_{max}^*\right) - \frac{4A\sigma_{GL}}{r_P\rho_L C_D\phi_1}L_{max}^* + \left\{\frac{4A\sigma_{GL}}{r_P\rho_L C_D\phi_1}\left(\frac{4\rho_a^*}{3C_D\phi_1}+1+\cos\theta\right)+\frac{8r_P g\rho_b^*}{3C_D\phi_1}\right\} \cdot \left\{1-\exp\left(-\frac{3C_D\phi_1}{4\rho_a^*}L_{max}^*\right)\right\} = 0 \quad (3)$$

The calculation results of the maximum penetration depth L_{max} $(= L_{max}^* \cdot r_P)$ by Equation (3) are shown in Fig. 8 by the solid line. These values were significantly smaller than the observed values in the present work. Even though the surface tension of the water is lower than that of the mercury used in the experiments by Ozawa et al., the same value of A was used in this calculation. Therefore, the influence of the interfacial tension may have been over-evaluated.

Then, another calculation was carried out on the assumption that no influence of interfacial tension is exerted. In this case, $\phi_3(x/r_P)$ equals 0 in Equation (1). Therefore, the particle movement can be expressed by Equation (4).

$$\frac{dv_P^2}{dx^*} + \frac{3C_D\phi_1}{4\rho_a^*}v_P^2 = \frac{2r_P g\rho_b^*}{\rho_a^*} \quad (4)$$

Equation (5) can be obtained by solving Equation (4) in the same critical condition as Equation (2).

$$L_{max} = \frac{4r_P\rho_a^*}{3C_D\phi_1}\ln\left(1-\frac{3C_D\phi_1 v_{P0}^2}{8r_P g\rho_b^*}\right) \quad (5)$$

The maximum penetration depth calculated by Equation (5) is shown in Fig. 8 by the broken line. It was larger than the observed values and did not agree with them. However, it was nearer to the observed values than the values calculated by Equation (3). This would indicate that the influence of interfacial tension is small, if any.

Moreover, defining particle velocity after penetration as v_{P0} (m/s), the maximum penetration depth was calculated by Equation (5). In this calculation, α was defined as 0.25, ϕ_1 as 1, ϕ_2 as 0.5, and C_D as 0.44 based on the assumption that a half part of a particle was dipped into liquid. As shown in **Fig. 9**, the calculated values almost agreed with the observed values. The maximum penetration depth may be almost governed by the particle velocity after penetration and may not be influenced by extension and rupture of the air column and the presence or absence of a residual bubble.

3.4 Diameter of residual bubble and average flotation velocity

The effect of particle velocity before penetration on the diameter of the residual bubble is shown in **Fig. 10**. The diameter of the residual bubble tended to increase with the increase in particle velocity before penetration. Also, as shown in **Fig. 11**, the diameter of the residual bubble correlated with the maximum air column length, H_{max}, except for experiment C1-3. It is assumed that as the particle velocity before penetration is higher, an air bubble is more easily generated and thereby more gas is involved in the water, which increases the diameter of the residual bubble.

The effect of the diameter of the residual bubble on the average flotation velocity of a particle is shown in **Fig. 12**. The particle with

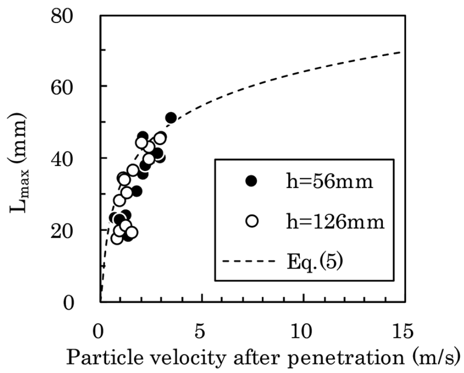

Fig. 9 Comparison of experimental results with calculated value about maximum penetration depth

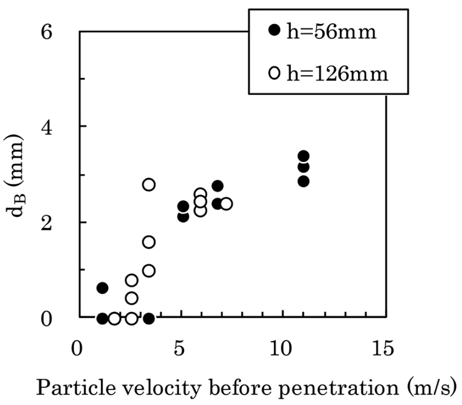

Fig. 10 Effect of particle velocity before penetration on diameter of residual bubble

a large residual bubble floated rapidly, indicating that the apparent density of the particle may be decreased by the residual bubble. The apparent density of a particle with a residual bubble, ρ_P'(kg/m^3), is given by Equation (6).

$$\rho_P' = \frac{d_P^3\rho_P + d_B^3\rho_B}{d_P^3 + d_B^3} \qquad (6)$$

Here, d_P is the diameter of the particle (m) and ρ_B is the density of the residual bubble (kg/m^3).

The terminal velocity of a particle moving in liquid, v_t, is expressed by Equations (7) to (9) corresponding to Reynolds number, Re.[14)]

$$\mathrm{Re}<6 \qquad v_t = \frac{g\Delta\rho d_P^2}{18\mu_L} \qquad \text{(Stokes's law)} \quad (7)$$

$$6<\mathrm{Re}<500 \qquad v_t = \left(\frac{4}{225}\cdot\frac{\Delta\rho^2 g^2}{\mu_L\rho_L}\right)^{\frac{1}{3}}\cdot d_P \qquad \text{(Allen's law)} \quad (8)$$

$$500<\mathrm{Re}<10^5 \qquad v_t = \left(\frac{3g\Delta\rho d_P}{\rho_L}\right)^{\frac{1}{2}} \qquad \text{(Newton's law)} \quad (9)$$

Where, $\Delta\rho\,(=\rho_L-\rho_P')$ is the difference in the density between the liquid and particles with the residual bubble (kg/m^3), and μ_L is the viscosity of the liquid (Pa·s).

The terminal velocity calculated by Equation (8), Allen's law, and Equation (9), Newton's law, is also shown in Fig. 12 by the broken line and the solid line, respectively. Terminal velocity calculated by Equation (7), Stokes's law, was not indicated because it was 0.5 to 4.5 m/s and Re (1 600 to 14 000) significantly exceeded the coverage of Stokes's law, Re<6.

The density of the residual bubble ρ_B is 0.85 kg/m^3 (density of Ar at 52 kPa, 20°C) and the viscosity of the water μ_L is 1.0×10^{-3}

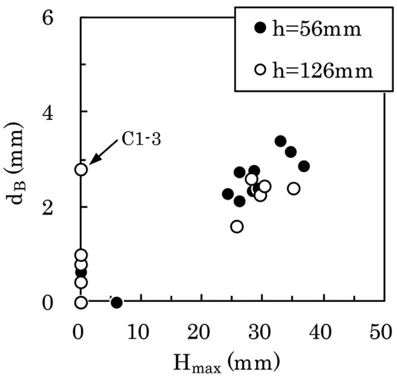

Fig. 11 Relation between maximum length of air column and diameter of residual bubble

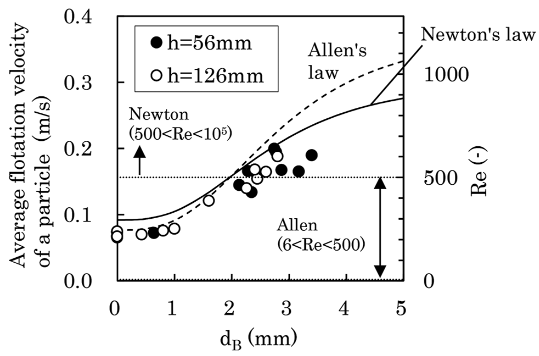

Fig. 12 Effect of diameter of residual bubble on average flotation velocity of a particle

Pa·s. The average flotation velocity of the particle followed Allen's law in the case that the diameter of the residual bubble was equal to or smaller than 2 mm, and followed Newton's law in the case that the diameter of the residual bubble was larger than 2 mm. The Reynolds number is indicated on the vertical axis on the right side in Fig. 12. The Reynolds number of the average flotation velocity of residual bubbles with a diameter of 2 mm is approximately 500, and it corresponds to the boundary between Allen's region and Newton's region. Therefore, the average flotation velocity measured in this investigation is valid.

3.5 Detention time of a particle

The relation between the particle velocity before the penetration and detention time of particles is shown in **Fig. 13**. The detention time of the particle in the cases that the particle velocity before penetration was equal to or higher than 3.4 m/s tended to become shorter than in the cases that the particle velocity before penetration was lower than 3.4 m/s. This is because when the particle velocity before penetration is equal to or higher than 3.4 m/s, a residual bubble with a diameter equal to or larger than 2 mm is easy to generate and the particle floats rapidly.

The relation between the maximum penetration depth and detention time of particles is shown in **Fig. 14**. The experimental data was separated into two groups based on the inclination of the diameters of the residual bubbles. One is indicated by the triangular marks in Fig. 14, corresponding to a residual bubble smaller than 1 mm in diameter. The other is indicated by the circular marks, corresponding to it being equal to or larger than 2 mm in diameter. When the residual bubble diameter is 1 to 2 mm, they are located between the two data groups. It suggests that the effect of increasing the detention time by increasing the maximum penetration depth is hardly obtained in the case of the particle with a residual bubble. Previous studies have mainly focused on the maximum penetration depth. However, the results in the present work indicate that blasting particles without generating a residual bubble is more important than increasing the maximum penetration depth by increasing the particle velocity before penetration. Factors that possibly affect the presence or absence of the air column and the residual bubble may be the wettability between the particle and liquid, pressure, particle diameter, and so forth. More investigation is necessary into how these factors affect the air column and the residual bubble.

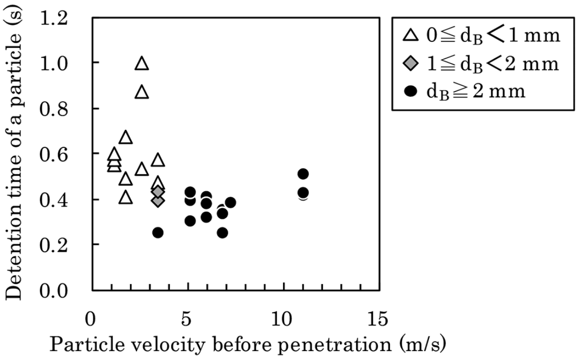

Fig. 13 Relation between particle velocity before penetration and detention time of a particle

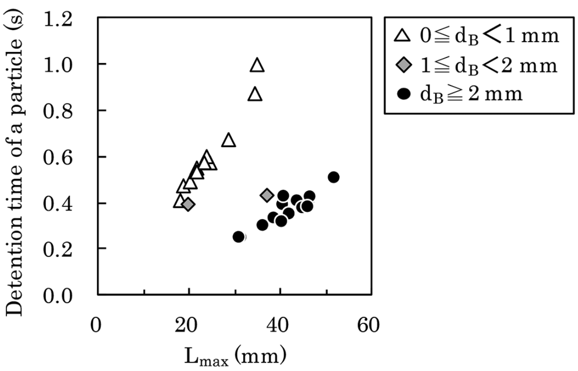

Fig. 14 Relation between maximum penetration depth and detention time of a particle

4. Conclusions

In order to clarify the effect of particle velocity on penetration and flotation behavior, a water model experiment by blasting a single particle onto the water surface was carried out. It was observed that an air column had been generated by the penetration of a particle and ruptured, a part of the ruptured air column had remained on the particle, and it became a residual bubble. The effect of the particle penetration velocity on the maximum penetration depth, diameter of the residual bubble, and detention time of the particle was analyzed. The following results were obtained in this investigation:

(1) The maximum penetration depth increases with the increase in particle velocity before penetration. The observed values of the maximum penetration depth almost agree with the calculated values of the kinetic equation where the particle velocity after penetration is used as the initial condition.

(2) The particle with high velocity before penetration easily generates a residual bubble, so it floats to the water surface rapidly, even though the maximum penetration depth is large. Blasting particles without forming a residual bubble is considered to be more important than increasing the maximum penetration depth by increasing particle velocity before penetration.

(3) The diameter of the residual bubble is correlated with the maximum air column length. To avoid generating a residual bubble, a particle has to be penetrated at a velocity at which no air column is generated.

References

1) Engh, T. et al.: Ironmaking Steelmaking. 6, 268 (1979)
2) Kimura, E.: Trans. Iron Steel Inst. Jpn. 23, 522 (1983)
3) Okuno, T. et al.: CAMP-ISIJ. 28, 656 (2015)
4) Narita, K. et al.: Tetsu-to-Hagané. 69 (3), 392 (1983)
5) Oda, T. et al.: Kobe Steel Eng. Rep. 56 (1), 32 (2006)
6) Ozawa, Y. et al.: Tetsu-to-Hagané. 69 (7), 753 (1983)
7) Lee, J. et al.: Trans. Iron Steel Inst. Jpn. 28, 278 (1988)
8) Shimamoto, N. et al.: Mater. Trans. 45 (3), 910 (2004)
9) Tanaka, M. et al.: J. Jpn. Soc. Exp. Mech. 8 (3), 201 (2008)
10) Duez, C. et al.: Nat. Phys. 3, 180 (2007)
11) Sakai, Y. et al.: Tetsu-to-Hagané. 98 (1), 1 (2012)
12) Edited by The Chemical Society of Japan (CSJ): Handbook of Chemistry: Pure Chemistry II. 3rd ed., Tokyo, Maruzen, 1991, p.81
13) Edited by The Chemical Society of Japan (CSJ): Handbook of Chemistry: Pure Chemistry II. 3rd ed., Tokyo, Maruzen, 1991, p.90
14) Mizushina, T. et al.: Chemical Engineering Outline. 1st ed., Tokyo, Sangyo Tosho Publishing, 2012, p.230

Akihiro MATSUZAWA
Senior Researcher
Muroran R & D Lab.
12 Nakamachi, Muroran City, Hokkaido 050-8550

Hiroshi HARADA
Chief Researcher, Dr. of Engineering
Canting-Rolling Research Lab.
Process Research Laboratories

Katsuhiro SASAI
Fellow, Head of Laboratories, Dr.Eng.
Process Research Laboratories

Mitsuhiro NUMATA
Chief Researcher, Dr. of Engineering
Nagoya R & D Lab.